Environment and Natural Resources Journal

Volume 25
Issue X
2027

Rainfall-Runoff Simulation and Hydrological Response Assessment using SWAT Model in an Urban Watershed

Priyanka Sharad Jawale[1,2*], Aruna Dattatraya Thube[1], and Kailas Arjun Patil[1]

[1]College of Engineering Pune Technological University, Pune, Maharashtra, India
[2]D. Y. Patil International University, Akurdi, Pune, India

ARTICLE INFO

Received: 7 Jan 2026
Received in revised: 7 Aug 2026
Accepted: 13 Aug 2026
Published online: 17 Nov 2026
DOI: 10.32526/ennrj/25/20260012

Keywords:
SWAT/ QSWAT/ Rainfall-runoff modelling/ Urban watershed/ Hydrological response/ Land use change/ Flood risk assessment

*** Corresponding author:**
E-mail:
priyankajawale29@gmail.com

ABSTRACT

Rapid urbanization and climate variability have substantially altered the hydrological response of urban watersheds, resulting in increased surface runoff, reduced infiltration, and a higher frequency of urban flooding. Understanding these changes is essential for sustainable watershed management and flood risk mitigation. This study evaluates the rainfall-runoff response of the Wakad urban watershed in the Mula River Basin, Pune, India, using the soil and water assessment tool (SWAT) implemented through the QSWAT interface. A high-resolution modelling framework was developed using a 30 m digital elevation model (DEM), 10 m land use/land cover (LULC) data, FAO soil data, and daily hydro-meteorological data obtained from NASA POWER for the period 1995-2023. The watershed was delineated into 28 sub-basins and corresponding hydrological response units (HRUs) to represent the spatial variability of terrain, land use, and soil characteristics. Model calibration and validation were performed using SWAT-CUP with the SUFI-2 algorithm. The calibrated model showed satisfactory performance, with a Nash-Sutcliffe Efficiency (NSE) of 0.72 and a coefficient of determination (R^2) of 0.78, indicating reliable simulation of streamflow. The simulation results revealed that increasing urbanization and expansion of impervious surfaces significantly increased surface runoff and reduced infiltration within the watershed. Peak runoff occurred during high-intensity monsoon events, with substantial temporal and spatial variability among sub-basins. The spatial distribution of runoff identified highly urbanized areas as being more susceptible to elevated runoff generation compared with relatively vegetated areas. The findings demonstrate the capability of the SWAT model to quantify long-term hydrological responses to land-use change in a rapidly urbanizing watershed. The study provides valuable hydrological information that can support watershed planning, flood risk assessment, and sustainable urban water resource management in rapidly developing cities.

HIGHTLIGHTS

- QSWAT simulated rainfall-runoff response in Wakad watershed from 1995-2023.
- Integrated 10 m LULC, 30 m DEM, and FAO soils supported spatially explicit HRU delineation.
- SUFI-2 calibration achieved NSE of 0.72 and R^2 of 0.78 for streamflow simulation.
- Model validation yielded NSE of 0.68 and R^2 of 0.74 with acceptable PBIAS.
- Spatial and temporal runoff diagnostics quantified seasonal and sub-basin variability.

1. INTRODUCTION

Urbanization is a significant driver of hydrological change in watersheds worldwide. The conversion of natural landscapes into impervious surfaces alters the natural water balance by reducing infiltration, increasing surface runoff, shortening runoff concentration time, and intensifying flood peak (Cross, 2001). These impacts are further aggravated by climate variability, particularly through changes in rainfall intensity and frequency, making urban flooding an increasingly serious environmental and socioeconomic challenge. Consequently, understanding the

Citation: Jawale PS, Thube AD, Patil KA. Rainfall-runoff simulation and hydrological response assessment using SWAT model in an urban watershed. Environ. Nat. Resour. J. 2027;25(X):xx-xx.

hydrological response of rapidly developing urban watersheds has become an important objective for sustainable urban planning and water resource management (Kron et al., 2012).

India has experienced rapid urban expansion over the past two decades, particularly in metropolitan regions such as Pune, where substantial land-use transformation has occurred owing to residential, commercial, and industrial development. The Wakad watershed, located within the Mula River Basin in Pune, India, has undergone considerable urban growth, resulting in the extensive replacement of permeable land with impervious surfaces. These land-use changes have modified runoff generation processes, increased stormwater volumes, and contributed to recurring flooding during the monsoon. Reliable hydrological modelling is therefore essential for understanding the effects of urbanization on watershed behavior and for supporting evidence-based planning and flood management strategies.

Physically based distributed and semi-distributed hydrological models have become valuable tools for evaluating watershed processes under changing environmental conditions. Among these, the soil and water assessment tool (SWAT) has been widely applied to simulate rainfall-runoff processes, water balance components, sediment transport, and land use impacts at the watershed scale. The QSWAT interface integrates SWAT with geographic information systems (GIS), enabling efficient watershed delineation, hydrological response unit (HRU) generation, and spatial analysis using topographic, soil, land use, and climatic datasets. Owing to its process-based structure and ability to represent spatial heterogeneity, SWAT has been successfully applied in numerous watershed studies worldwide.

Previous studies have demonstrated the effectiveness of SWAT in evaluating the impacts of land use change and climate variability on watershed hydrology. However, many applications have focused primarily on agricultural or mixed land use catchments, while relatively few studies have investigated highly urbanized watersheds characterized by extensive impervious cover and rapid land use transformation. Furthermore, many studies have relied on coarse spatial datasets or relatively short simulation periods, limiting their ability to capture long-term hydrological changes associated with sustained urban growth.

The Wakad watershed provides an appropriate case study for investigating these processes because of its rapid urbanization and increased flood vulnerability. High-resolution spatial datasets combined with long-term hydrometeorological records offer an opportunity to evaluate how urban development has influenced rainfall-runoff relationships and spatial runoff distribution over time (Vázquez-Tarrío et al., 2024). Such analyses contribute to a better understanding of hydrological processes in urban environments and provide information that supports sustainable watershed management in the region.

The objectives of this study are as follows:

1. Develop a high-resolution QSWAT model of the Wakad urban watershed using DEM, land use, soil, and hydro-meteorological datasets.

2. The SWAT model was calibrated and validated using the SWAT-CUP SUFI-2 algorithm, and the model performance was evaluated using standard statistical indicators.

3. Assess the long-term rainfall-runoff response of the watershed during the period 1995-2023.

4. Analyze the influence of land use characteristics and watershed physiography on spatial runoff generation.

5. It provides hydrological information that supports watershed management and urban flood risk assessment.

2. METHODOLOGY

2.1 Study area

The Wakad watershed is located within the Pimpri-Chinchwad Municipal Corporation (PCMC), Pune District, Maharashtra, India, and is part of the Mula River Basin. The watershed covers an area of approximately 603.446 ha and has experienced rapid urbanization over the past two decades owing to the extensive development of residential, commercial, and transportation infrastructure. The conversion of natural and agricultural land into impervious urban surfaces has substantially altered the hydrological response of watersheds, resulting in increased surface runoff and greater susceptibility to urban flooding during the southwest monsoon season (Ghosh and Guchhait, 2016).

The watershed is bounded by latitudes 18.58°-18.61°N and longitudes 73.75°-73.78°E. The drainage system ultimately conveys runoff to the Mula River, while the upstream Mulshi Reservoir influences downstream flow conditions during periods of

regulated releases. However, the present study primarily focuses on rainfall-runoff simulation within the watershed using the SWAT model. The combination of rapid urban growth, relatively small watershed area, and increasing flood occurrences makes the Wakad watershed an appropriate case study for evaluating long-term hydrological responses under changing land-use conditions. Figure 1 shows the spatial extent of the Wakad watershed, its boundary, stream network, and geographic reference system that will be used to analyze the hydrology of the watershed, and Figure 2 depicts the 28 sub-basins that are automatically created in QSWAT according to terrain features and stream connectivity, which are the units of space in which the routing of hydrological processes takes place.

2.2 Data collection and preparation

The SWAT model requires topographic, land use, soil, and hydro-meteorological datasets for watershed characterization and rainfall-runoff simulation. The datasets used in this study are presented in Table 1.

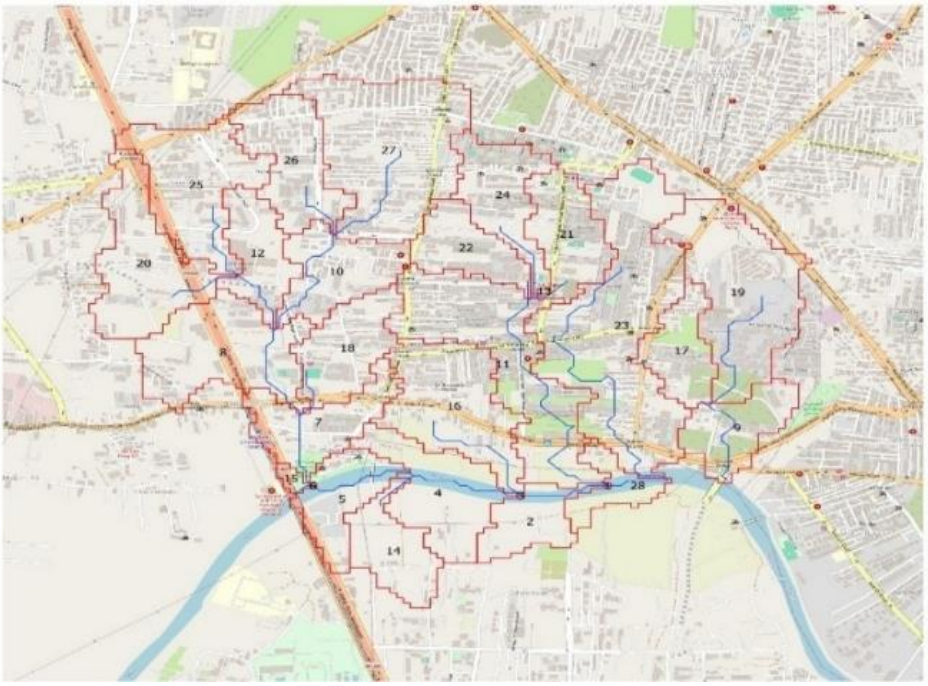


Figure 1. The watershed of Wakad and the QSWAT categorized them into sub-basin for easier identification (source: NASA earth data)

Table 1. Spatial and hydrometeorological datasets used in SWAT modelling

Dataset	Source	Resolution/period	Purpose
Digital elevation model (DEM)	NASA earth data	30 m	Watershed delineation and slope generation
Land use/land cover	Esri ArcGIS living Atlas	10 m	HRU generation
Soil map	FAO digital soil map	Global	Soil parameterization
Meteorological data	NASA POWER	Daily (1995-2023)	Rainfall and climatic inputs
Streamflow data	Observed discharge	Calibration and validation	Model evaluation

The DEM was used to delineate the watershed boundary, derive the stream network, and generate slope classes. The DEM had a spatial resolution of approximately 30.05×30.05 m, which is considered to have an adequate granularity to capture the subtle differences in elevation that affect micro-scale hydrological processes within an urban setting. Daily rainfall, temperature, solar radiation, humidity, and wind speed data obtained from NASA POWER were formatted according to the SWAT input requirements after quality control and preprocessing. The resulting processed DEM (Figure 3) has high fidelity in terms of capturing the elevation gradients of the watershed, which is consistent with the accurate simulation of runoff distribution and sub-basin hydrological response.

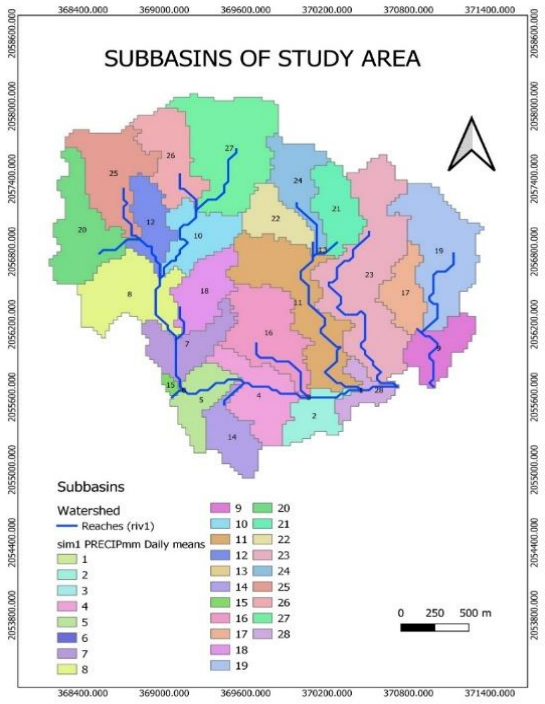


Figure 2. Sub-basins and stream network in the Wakad catchment. The above catchment consists of 28 sub-basins. (source: NASA earth data and QGIS)

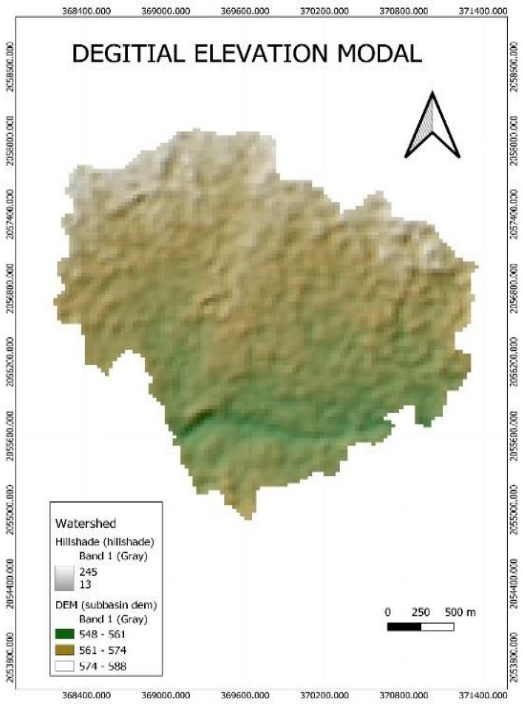


Figure 3. Digital elevation model with a 30-m resolution specifically tailored to the Wakad catchment area (source: NASA earth data and QGIS)

2.3 SWAT model description

The Soil and Water Assessment Tool (SWAT) is a semi-distributed, process-based hydrological model developed by the United States Department of Agriculture (USDA) to simulate the effects of land management and climatic variability on watershed hydrology. The model divides a watershed into multiple sub-basins, which are further subdivided into HRUs representing unique combinations of land use, soil type, and slope (Wang et al., 2019).

SWAT estimates the water balance using the following equation:

$$SW_t = SW_0 + \sum_{\{i=1\}}^{t} \left(R_i - Q_{\{surf\}} - ET_i - W_{\{seep\}} - Q_{\{gw\}}\right)$$

Where; SW_t=final soil water content (mm); SW_0=initial soil water content (mm); R_i=precipitation (mm); Qsurf=surface runoff (mm); ET_i= evapotranspiration (mm); W_{seep}=percolation (mm); Q_{gw}=groundwater flow (mm).

This water balance forms the basis for simulating rainfall-runoff processes within each HRU before routing flows through the stream network.

2.4 Watershed delineation and HRU generation

Watershed delineation was performed using the QSWAT interface in QGIS. The processed DEM was used to generate flow direction, flow accumulation, and stream network layers, from which the watershed boundary and sub-basins were automatically delineated.

The delineated watershed comprised 28 sub-basins. Hydrological response units (HRUs) were subsequently generated by overlaying land-use, soil, and slope datasets as shown in Figure 4. HRUs represent homogeneous hydrological units and enable SWAT to simulate runoff generation while accounting for spatial variability in watershed characteristics (Motsinger et al., 2016).

2.5 Land use/land cover results

The Wakad watershed is highly urbanized, with urban land covering 90.52% of the area, as shown in Figure 5. This high imperviousness results in reduced infiltration and recharge, higher runoff volumes and velocities, sharper hydrographs, and increased flood vulnerability during monsoon periods (Ogden et al., 2001). Although forest (0.20%) and rangeland (2.46%) areas are limited, they serve as important ecological buffers.

Urban expansion has also reduced agricultural land (6.06%), further diminishing natural runoff attenuation. Overall, urban sprawl is the dominant driver of increased runoff magnitude and frequency.

Table 2 gives a summary of the area occupied by each land-use category in the watershed and its relative contribution to the hydrological behaviour.

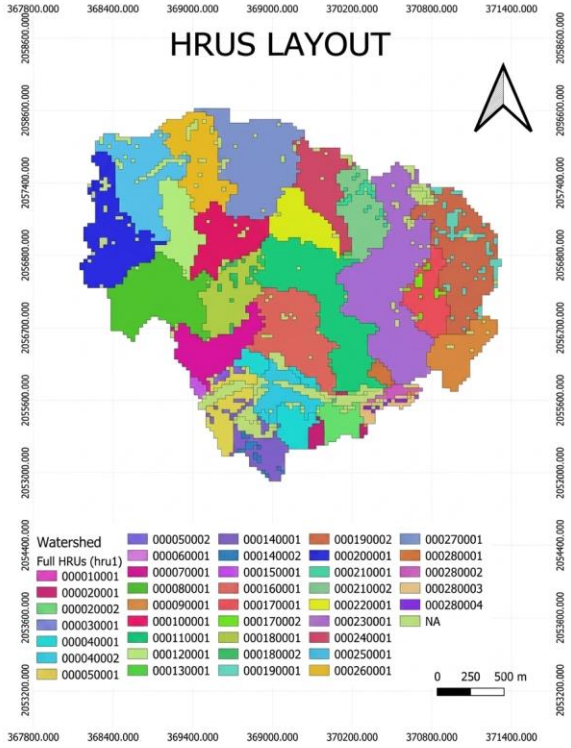


Figure 4. HRU result from LULC, soil map and slope map (source: QSWAT and Esri ArcGIS living 10 m)

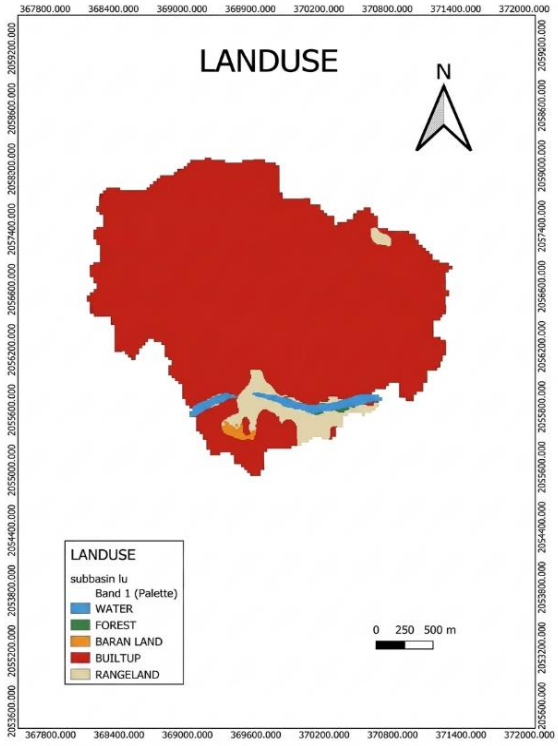


Figure 5. Land use classification (source: land use (raster) from Esri ArcGIS living 10 m LULC map)

Table 2. Area occupied by each land-use category in the watershed

Land use	Abbreviation	Area (ha)	Area (acres)	%wat. area
Water body	WATR	4.58	11.31	0.76
Forest	FRST	1.21	2.99	0.20
Urban	URBN	546.11	1,348.89	90.52
Agriculture	AGRR	36.81	90.92	6.06
Range land	RNGE	15.08	37.24	2.46

2.6 Soil classification results

The watershed was represented by a single soil type (Vc43-3ab), covering 100% of the area. This homogeneity reduced parameter uncertainty and allowed clearer attribution of hydrological change to land-use and climate effects rather than soil variability. Although the soil was moderately well-drained, urban surface sealing limited infiltration, making anthropogenic factors the primary control on watershed hydrology. Figure 6 shows the distribution of soil type in the watershed that was modeled in QSWAT for infiltration and water storage.

Table 3 shows the soil classification applied in the model and the area covered by each soil unit in the watershed.

2.7 Slope range classification results

Slope analysis indicates the dominance of gentle to moderate slopes, with 0-2% covering approximately 48.3% and 2-4% covering 38.6% of the watershed. Gentle slopes facilitate rapid runoff transfer to drainage systems in urban areas, whereas steeper sections (>4%) accelerate runoff during heavy rainfall. These results confirm the role of micro-topography in shaping runoff response in small urban

watersheds (Shukla and Gedam, 2019). The slope classes in Figure 7 are based on the DEM and reflect the variation in the terrain and its impact on the overland flow velocities within the watershed.

Table 4 shows the slope ranges in the study area and their respective spatial coverage, which is an effect of the terrain on runoff generation.

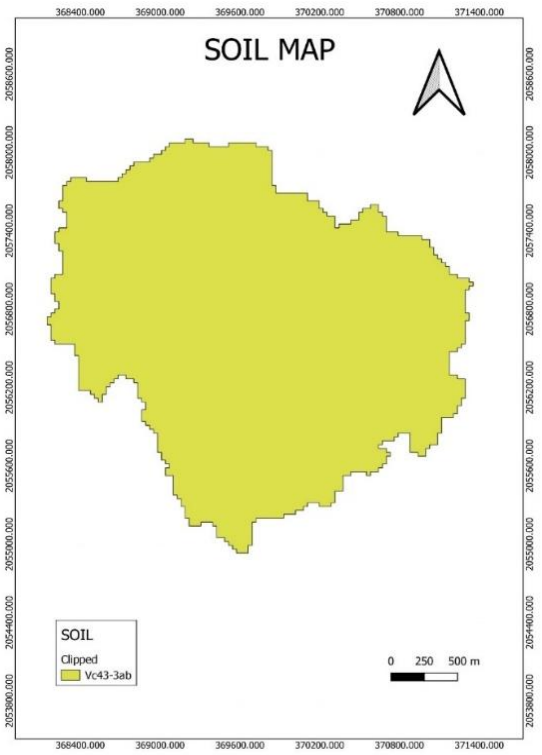


Figure 6. Soil types classification (source: Food and Agriculture Organization of the United Nation (FAO))

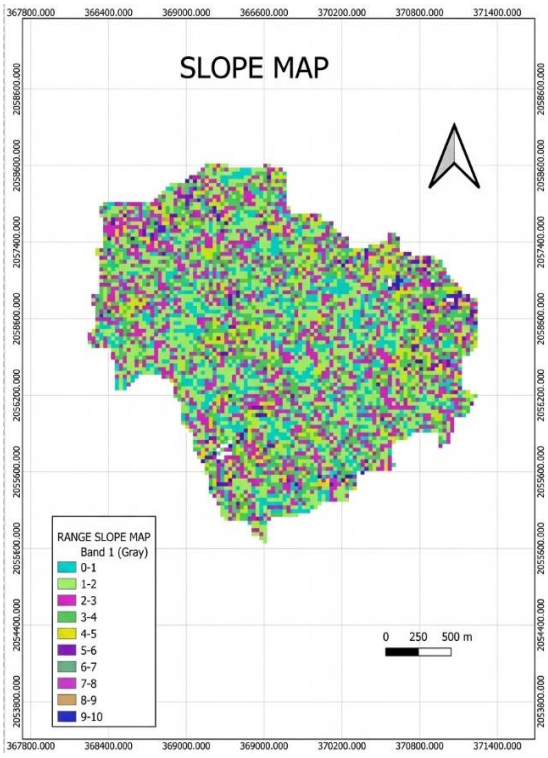


Figure 7. Slope map of Wakad Catchment (source: QGIS and QSWAT database)

Table 3. Soil types result (source: Food and Agriculture Organization of the United Nation (FAO))

Soil	Area (ha)	Area (acre)	%wat. Area
Vc43-3ab	603.47	1491.15	100

Table 4. Slope range results (source: QGIS and QSWAT database)

Slope	Area (ha)	Area (acres)	%wat. area
0-1	99.56	245.91	16.49
1-2	191.89	472.96	31.77
2-3	146.63	362.17	24.29
3-4	86.29	213.13	14.27
4-5	45.25	111.76	7.48
5-6	16.89	41.71	2.80
6-7	9.05	22.35	1.47
7-8	4.34	10.71	0.72
8-9	2.41	5.95	0.37
9-10	1.87	4.61	0.31

2.8 Precipitation trends

Rainfall analysis shows an increasing trend in average annual rainfall over the 28-year period, with greater inter-annual variability and periodic extreme years. Although the absolute values are low due to POWER data averaging, the trend indicates wetter monsoon seasons and increased rainfall intensity, which is a key contributor to runoff escalation

(Tanksali and Soraganvi, 2021). These patterns align with regional IMD observations.

Figure 8 shows the long-term rainfall pattern, which is variable and shows a rise in the intensity of rainfall throughout the simulation period.

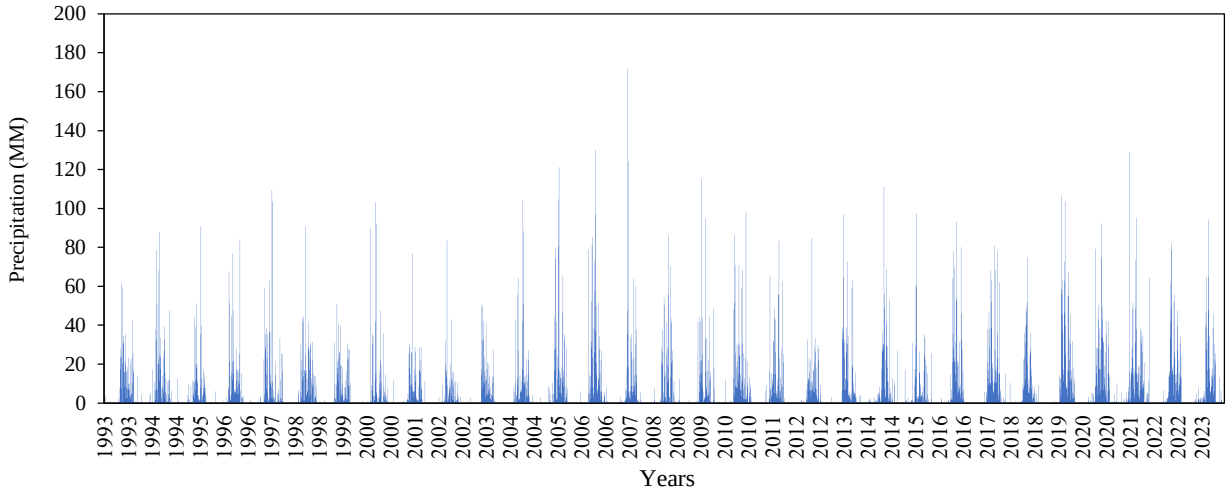


Figure 8. Average annual rainfall (source: NASA POWER (predication of worldwide energy resource) and IMD department, Pune Dist.)

2.9 Model setup

The simulation period extended from January 1995 to December 2023, with the initial two years used as a warm-up period to minimize the influence of the initial model conditions. Daily climatic inputs, including rainfall, maximum and minimum temperatures, relative humidity, solar radiation, and wind speed, were incorporated into the model (Gong et al., 2024). The default SWAT parameters were initially adopted and subsequently refined through calibration.

2.10 Model calibration and validation

Model calibration and validation were performed using SWAT-CUP with the sequential uncertainty fitting version 2 (SUFI-2) algorithm. Approximately 70% of the observed discharge data were used for calibration, andthe remaining 30% were reserved for validation.

The calibration focused on sensitive hydrological parameters, including:

- Curve number (CN2)
- Available water capacity (SOL_AWC)
- Baseflow alpha factor (ALPHA_BF)
- Channel manning's roughness (CH_N2)
- Soil evaporation compensation factor (ESCO)

Parameter optimization was performed iteratively until acceptable agreement between the observed and simulated streamflow was achieved (Di Luzio et al., 2002).

3. RESULTS AND DISCUSSION

3.1 Model calibration and validation

The performance of the SWAT model was evaluated using SWAT-CUP software with the SUFI-2 calibration algorithm (Dixon and Earls, 2012). The model was calibrated using observed streamflow data and subsequently validated using an independent dataset. Model performance was assessed using the Nash-Sutcliffe Efficiency (NSE), coefficient of determination (R^2), percent bias (PBIAS), and root mean square error-observation standard deviation ratio (RSR).

The calibrated model achieved an NSE of 0.72 and an R^2 value of 0.78, indicating satisfactory agreement between the observed and simulated streamflow, as shown in Table 5. The statistical performance demonstrates that the model adequately represents the hydrological behavior of the Wakad watershed and is suitable for long-term rainfall-runoff simulation.

The calibration process also reduced systematic prediction errors by optimizing sensitive hydrological parameters, including the CN2, available water capacity (SOL_AWC), baseflow alpha factor (ALPHA_BF), and channel Manning's roughness coefficient (CH_N2) (Quiroga et al., 2011). SUFI-2 sensitivity analysis identifies CN2 as the most sensitive parameter, as indicated in Table 6, emphasizing the role of imperviousness and land use in runoff generation. Parameters related to baseflow and soil moisture show moderate sensitivity, reflecting

reduced groundwater influence in urbanized setting (Nainwal, 2021).

Overall, the calibration and validation results indicate that the developed SWAT model provides a reliable basis for evaluating long-term hydrological responses under changing land use and climatic conditions (Shiferaw et al., 2025).

Table 5. Model performance statistics for calibration and validation periods

Metric	Calibration	Validation	Interpretation
NSE	0.72	0.68	Acceptable to good performance (Moriasi et al., 2015)
R^2	0.78	0.74	Strong statistical agreement
PBIAS	+6.3%	+9.2%	Within acceptable ±25% range
RMSE	18.2 m^3/s	21.7 m^3/s	Slightly higher errors during extreme events

Table 6. Sensitivity ranking of calibrated SWAT parameters

Rank	Parameter code	Description	Sensitivity level	Hydrological influence
1	CN2	SCS curve number	Very high	Controls surface runoff and infiltration partitioning
2	ALPHA_BF	Baseflow alpha factor	High	Governs groundwater recession and sustained flow
3	SOL_AWC	Soil available water capacity	High	Influences soil storage and storm response
4	GW_DELAY	Groundwater delay time	Medium	Affects timing of groundwater contribution
5	CH_N2	Manning's n for main channel	Medium	Controls flow routing and discharge velocity
6	ESCO	Soil evaporation compensation factor	Low	Impacts evapotranspiration and moisture availability
7	GW_REVAP	Groundwater-soil revap coefficient	Low	Minor influence on baseflow return flow

3.2 Rainfall-runoff simulation

The calibrated SWAT model was used to simulate rainfall-runoff processes from 1995 to 2023. The simulation results indicate considerable temporal variability in runoff generation, reflecting variations in annual rainfall and progressive urbanization within the watershed (Yohannes et al., 2024). Peak runoff was consistently associated with the southwest monsoon season, particularly during June to September, when intense rainfall events generated rapid surface runoff (Hadachek et al., 2026). Monthly averaged outputs show strong seasonal contrasts, with minimal runoff during the pre-monsoon months and pronounced peaks during the monsoon (Table 7).

The simulated surface runoff in the watershed is spatially presented in Figure 9, and the hotspots of runoff and drainage concentration areas are indicated.

Figure 10 shows the simulated discharge at the watershed outlet, which is seasonally variable and monsoon-influenced peak flows.

Table 8 presents the long-term monthly simulated runoff, which indicates seasonal and interannual hydrological variability.

Table 7. Average simulation monthly basin value (source: NASA POWER (prediction of worldwide energy resource) and QSWAT)

Month	Rainfall (mm)	ET (mm)	PET (mm)	Sediment (Tons)	Surface runoff (Q) (mm)
1	0.063	14.249	95.475	0.279	0.173
2	0.056	21.788	119.253	0.072	0.135
3	0.125	53.532	172.490	0.024	0.256
4	0.179	22.682	178.919	0.019	0.311
5	1.185	28.909	155.008	0.833	7.746
6	11.348	52.402	87.931	39.210	125.532
7	17.107	58.845	74.511	124.251	269.127
8	11.741	55.337	69.040	101.804	168.301
9	8.996	48.552	65.449	79.956	116.505
10	3.561	43.603	90.774	33.480	39.392
11	0.802	27.499	101.261	6.746	5.635
12	0.256	18.128	92.425	2.917	2.647

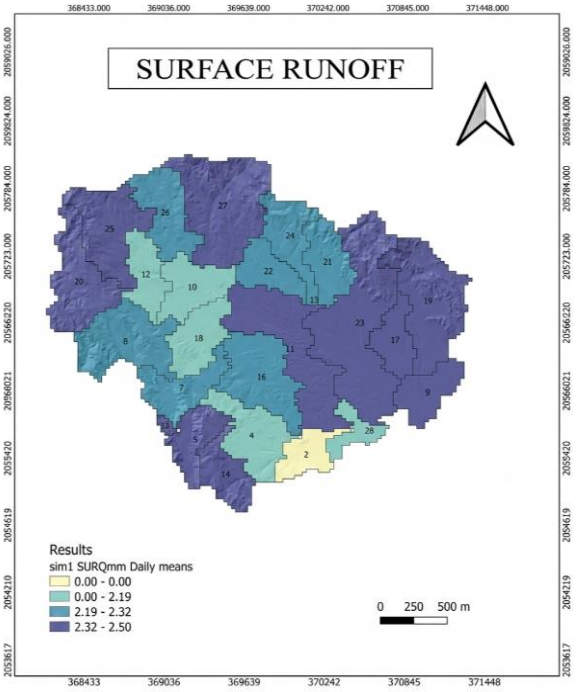


Figure 9. Surface runoff map (Source: QSWAT and NASA POWER)

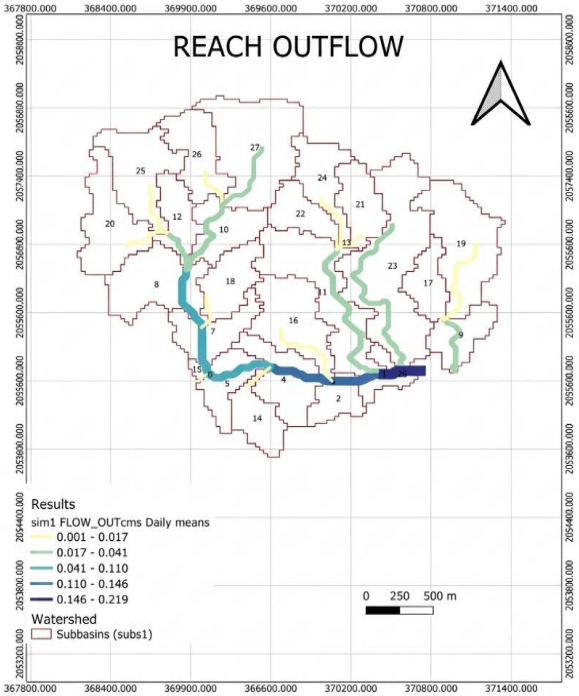


Figure 10. Reach outflow (Source: QSWAT and NASA POWER)

Table 8. Monthly surface runoff from year 1995 to 2023 (source: QSWAT and NASA POWER)

Year	Jan	Feb	Mar	Apr	May	Jun	Jul	Aug	Sep	Oct	Nov	Dec
1995	53.265	0	0	36.216	29.582	344.91	982.5	506.1	1882.7	165.65	0	0
1996	0	16.197	0	0.154	3.188	903.2	1579.4	408.1	366.2	1670.3	5.1377	0
1997	0.634	0	0	3.188	3.8162	646	1236	2296.3	223.56	20.558	493	323.4
1998	0	0	0	0	19.144	547.5	1842.6	797.8	474.3	481.5	101.58	0
1999	0	0.246	0	0	180.92	611.9	683.1	217.09	467.3	426.7	0.000	0
2000	0	0.004	0	0	1027.5	544.8	2083.4	868.1	490.6	144.7	25.612	46.353
2001	3.299	0	0	0	11.61	387.8	1567.7	464.3	415.6	473.6	47.553	0
2002	0	0	0	3.491	34.535	1677.1	106.3	747.2	179.62	60.4	4.1211	0
2003	0	3.491	0	0	0	775.8	714.2	289.9	145.3	358.9	0.004	0
2004	0	0	0	0	316.71	1212.7	774.8	2253.3	393.6	9.682	8.160	0
2005	3.717	0.266	0	28.522	39.583	1575.8	2049.2	2658	1294.3	365	0.000	0
2006	0	0	14.767	0	967.5	1002.1	1814.6	2761	911.9	423.9	25.853	0
2007	0	0	0	4.454	0.246	3206	2632	1214.2	1081.4	0.983	14.825	0
2008	0	0	23.538	0	2.617	990.6	764.9	1801.9	1387.7	72.9	8.57	54.735
2009	0	0	0.35742	0	0.032	339.86	2441.5	1879.6	515.4	855.7	722.8	0
2010	0	0	46.438	0	62.915	1420.4	1513.7	1356.6	363.5	1962.7	83.08	0
2011	0	0	0	34.714	1.838	703.9	964.9	1111.7	1700.5	1132.8	0.001	0
2012	0	0	0	0.251	0.032	201.61	1705.3	655.3	538.1	445	0.032	0
2013	0	3.802	0	0	0	2074	1440.4	588.4	1190.7	169.42	4.790	6.979
2014	0	0.246	1.602	3.802	8.982	28.319	2453.2	1374.7	943.2	74.46	56.959	223.04
2015	0	65.354	89.82	0.0012	182.03	2029.2	400	47.49	561.4	245.17	275.02	0
2016	0	0.154	2.617	0	0.668	873	1579	2029.4	1636.4	378.9	0	0
2017	0	0	0	0	14.767	837.8	1355.3	1596	1638.5	1163.7	2.897	83.35
2018	37.899	0	0	0	0.797	661	1540.3	626.8	140.94	25.042	36.469	0
2019	0	0	0	0.032	14.697	1890.9	1946.6	2251.2	1689.1	445.2	128.61	0
2020	0	0	3.491	0.2461	12.013	857.9	933.6	1899.5	738.7	758.8	0	9.4
2021	36.809	13.252	2.346	13.836	1774.5	1020.3	1991.2	635.8	637.5	262.35	65.48	1047.9
2022	0	0	0	17.167	1.602	375.3	1763.4	1115.7	854	554	0	0
2023	0	0	9.82	25.845	4.013	1193.7	2054.3	213.08	868	379.9	63.61	0.797

3.3 Inter-annual variability and peak events

Significant inter-annual variability was observed, with extreme runoff years such as 2007 and 2019. The highest monthly runoff occurred in June 2007 (3,206 mm), likely amplified by reservoir releases under moderate rainfall, highlighting the upstream control effects. Seasonal patterns indicate minimal runoff during the pre-monsoon months, extreme runoff during the monsoon, and delayed drainage post-monsoon (Bisimwa et al., 2025).

3.4 Long-term runoff escalation

Runoff shows an increasing long-term trend owing to urban growth, intensified rainfall, modified channels, and reservoir-storm interactions. Peak flood months are consistently June and July, with occasional extremes in May and December linked to reservoir operations (Meer, 2026). The average monthly runoff peak was in July, while mean annual runoff nearly doubledduring extreme years, such as 2019. The increase in impervious surfaces reduced infiltration opportunities and accelerated surface runoff, resulting in greater runoff volumes during monsoon events (Ansari et al., 2025). Seasonal analysis further indicated that mostrunoff occurred during the southwest monsoon season, while comparatively low runoff was observed during the remaining months. The long-term hydrological assessment highlights the cumulative influence of land use change and rainfall variability on watershed response and demonstrates the importance of continuous hydrological monitoring in rapidly urbanizing catchments (Albarico et al., 2026).

Figure 11 shows the distribution of the maximum monthly surface runoff over time and the years of extreme hydrological years, and the storm events are identified.

Table 9 shows the highest amount of surface runoff per month and year of occurrence, which demonstrates extreme hydrological conditions.

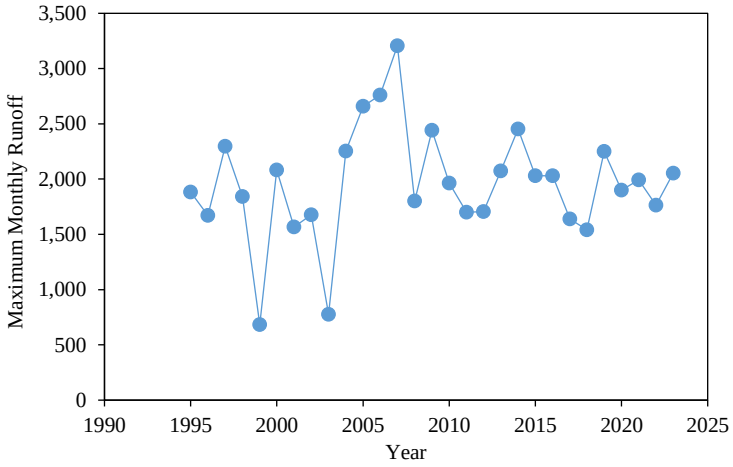


Figure 11. Maximum monthly runoff graph (Source: QSWAT)

Table 9. Maximum monthly surface runoff and its water year of occurrence (Source: QSWAT)

Month	Maximum surface runoff (mm)	Water year of occurrence
January	53.265	1995
February	65.354	2015
March	89.820	2015
April	36.216	1995
May	1,774.500	2021
June	3,206.000	2007
July	2,632.000	2007
August	2,761.000	2006
September	1,882.700	1995
October	1,962.700	2010
November	722.800	2009
December	1,047.900	2021

In addition, the 2007 event-based analysis supports the fact that the single-month extremes prevail in the flood-generating mechanism in this watershed.

Table 10 shows the monthly distribution of runoff in the extreme year of flood in the simulation period (2007).

3.5 Average monthly runoff trends

It is found that:

- The maximum average runoff (269.13 mm) was recorded in July.
- The mean runoff was 61.77 mm/per year although the values almost doubled during extreme years.

Figure 12 shows the mean monthly runoff patterns, which show a seasonal concentration of runoff during the monsoon months.

Table 11 presents the monthly runoff in 2019, a recent year with high flood response owing to increased monsoon activity.

3.6 Highlights of the major results of the simulation

- Over the past 30 years, there has been tremendous growth in runoff.
- Extreme runoff (e.g., 2007, 2010, 2019) is associated with an interplay of rainfall intensity, urbanization, and dam releases.
- HRU-based modeling clearly shows that urban imperviousness is the primary contributor to runoff volume.
- Seasonal dynamics indicate that the potential of annual floods is determined by the monsoon peaks, and the dry season flow is insignificant.

Slope and soil characteristics are secondary modifiers, with urban land cover being the most important.

3.7 Future work, limitations, and recommendations

While QSWAT showed good performance, its limitations include the use of daily NASA POWER rainfall data, which cannot resolve sub-hourly convective storms; simplified representation of urban drainage networks; limited streamflow observations; and estimated dam operation schedules (Mishra et al., 2025). Future work should integrate high-resolution radar rainfall, real-time gauging, coupled SWAT-SWMM or hydrodynamic models, verified dam release data, and scenario-based land useand climate projections. Incorporating groundwater monitoring and socioeconomic exposure modeling would further enhance decision-support capability.

Table 10. Monthly maximum runoff of water year 2007 (Source: QSWAT)

Month	Year 2007
January	0
February	0
March	0
April	4.454
May	0.246
June	3,206.000
July	2,632.000
August	1,214.200
September	1,081.400
October	0.983
November	14.825
December	0
Maximum runoff	3,206.00

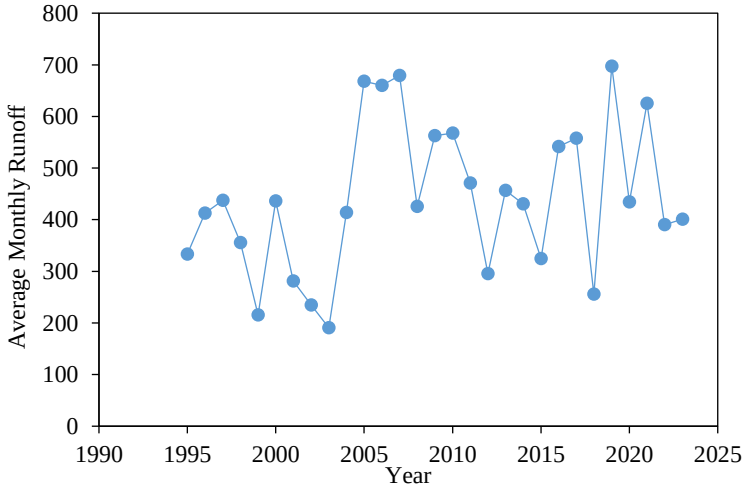


Figure 12. Average monthly runoff graph (Source: QSWAT and NASA POWER)

Table 11. Average monthly runoff value for water year 2019 (Source: QSWAT) (cont.)

Month	Year 2019
January	0
February	0
March	0
pril	0.032
May	14.697
June	1,890.900
July	1,946.600
August	2,251.200
September	1,689.100
October	445.200
November	128.610
December	0
Average annual runoff	697.194

4. CONCLUSION

The rainfall-runoff characteristics simulated by the SWAT model are consistent with previous studies reporting increased runoff generation in urban watersheds owing to the expansion of impervious surfaces and reduction of natural infiltration (Bayissa et al., 2025). The long-term simulation confirmed that urban growth significantly altered the hydrological response of the Wakad watershed, leading to greater runoff volumes and increased flood susceptibility during high-intensity rainfall events.

The use of high-resolution land-use data and detailed hydrological response units (HRUs) enabled an improved representation of spatial heterogeneity within the watershed, contributing to satisfactory model performance. Although the SWAT model effectively simulated watershed-scale rainfall-runoff processes, it does not explicitly represent underground urban drainage networks or storm sewer systems. Therefore, the present study should be interpreted as providing watershed-scale hydrological information rather than detailed urban drainage analysis.

The findings of this study can support watershed management, urban planning, and future investigations integrating hydrological models with hydraulic or stormwater drainage models for comprehensive flood prediction.

ACKNOWLEDGEMENTS

The authors also admit that they used an open-source dataset and tools, which enabled them to do so: NASA Earth Data (DEM), NASA POWER climatic products, FAO soil maps, and Esri ArcGIS LULC resources. Local knowledge and partial operational information (where available) were courtesy of the Pimpri-Chinchwad Municipal Corporation. The QSWAT and SWAT-CUP systems played a significant role in the development and calibration of the models. Any mistakes left behind are the prerogative of the authors.

AUTHOR CONTRIBUTIONS

Conceptualization, Methodology, Investigation, Data Curation, Formal Analysis, Visualization, Writing-Original Draft, P.S.J.; Supervision, Methodology, Validation, Writing-Review and Editing, A.D.T.; Supervision, Validation, Writing-Review and Editing, K.A.P.

DECLARATION OF CONFLICT OF INTEREST

The authors declare that they have no known competing financial interests or personal relationships that could have influenced the work reported in this study.

REFERENCES

Albarico FPJB, Chen CW, Dong CD. Multifactorial environmental and ecological gradients from hydrology and land-use reflect coordinated plankton-organic pollutant spatial dynamics in coastal ecosystems. Water Research 2026;288(Pt B):Article No. 124727.

Ansari A, Timilsina AP, Shah A, Manandhar A, Khanal S. Switchgrass for abandoned mine lands reclamation: A SWAT-based hydrological and water quality assessment. Agricultural Water Management 2025;318:Article No. 109730.

Bayissa Y, Srinivasan R, Hunink J, Nyolei D, Moges S, Costa DDA, et al. Evaluating the potential of nature-based solutions to mitigate land use and climate change impacts on the hydrology of the Gefersa and Legedadi watersheds in Ethiopia. Journal of Hydrology: Regional Studies 2025;57: Article No. 102130.

Bisimwa AM, Hwaba M, Akuzwe D, Guesri M, Muhaya BB, Kankonda AB. Effects of land use-land cover changes on hydrology and sediment transport in Bukavu urban river catchments, Lake Kivu Basin, Democratic Republic of the

Congo. Journal of Great Lakes Research 2025;51(6):Article No. 102700.

Cross JA. Megacities and small towns: Different perspectives on hazard vulnerability. Global Environmental Change Part B: Environmental Hazards 2001;3(2):63-80.

Di Luzio M, Srinivasan R, Arnold JG. Integration of watershed tools and SWAT model into BASINS. Journal of the American Water Resources Association 2002;38(4):1127-43.

Dixon B, Earls J. Effects of urbanization on streamflow using SWAT with real and simulated meteorological data. Applied Geography 2012;35(1-2):174-90.

Ghosh S, Guchhait SK. Dam-induced changes in flood hydrology and flood frequency of a tropical river: A study of the Damodar River, West Bengal, India. Arabian Journal of Geosciences 2016;9(2):Article No. 90.

Gong Y, Geng X, Wang P, Hu S, Wang X. Impact of urbanization-driven land use changes on runoff in the upstream mountainous basin of Baiyangdian, China: A multi-scenario simulation study. Land 2024;13(9):Article No. 1374.

Hadachek J, Mérel P, Somerville S. The impact of land use on water quality: Evidence from California wells. Journal of Environmental Economics and Management 2026;137:Article No. 103284.

Kron W, Steuer M, Löw P, Wirtz A. How to deal properly with a natural catastrophe database-analysis of flood losses. Natural Hazards and Earth System Sciences 2012;12(3):535-50.

Meer MS. Spatiotemporal dynamics of land use change and agrochemical-driven water quality degradation. Desalination and Water Treatment 2026;325:Article No. 101582.

Mishra VK, Khalkho D, Kumar A, Kumar L, Gloria M. Machine learning driven assessment of climate and land use change impacts on water resources in the Kharun River Basin, Central-Eastern India. Environmental and Sustainability Indicators 2025;28:Article No. 101031.

Motsinger J, Kalita P, Bhattarai R. Analysis of best management practices implementation on water quality using the soil and water assessment tool. Water 2016;8(4):Article No. 145.

Nainwal A. Water resource management for sustainable urban development. Mathematical Statistician and Engineering Applications 2021;70(1):706-12.

Ogden FL, Garbrecht J, DeBarry PA, Johnson LE. GIS and distributed watershed models. II: Modules, interfaces, and models. Journal of Hydrologic Engineering 2001;6(6):515-23.

Quiroga S, Garrote L, Iglesias A, Fernández-Haddad Z, Schlickenrieder J, De Lama B, et al. The economic value of drought information for water management under climate change: A case study in the Ebro Basin. Natural Hazards and Earth System Sciences 2011;11(3):643-57.

Shiferaw N, Habte L, Waleed M. Land use dynamics and their impact on hydrology and water quality of a river catchment: A comprehensive analysis and future scenario. Environmental Science and Pollution Research 2025;32(7):4124-36.

Shukla S, Gedam S. Evaluating hydrological responses to urbanization in a tropical river basin: A water resources management perspective. Natural Resources Research 2019;28(2):327-47.

Tanksali A, Soraganvi VS. Assessment of impacts of land use/land cover changes upstream of a dam in a semi-arid watershed using QSWAT. Modeling Earth Systems and Environment 2021;7(4):2391-406.

Vázquez-Tarrío D, Ruiz-Villanueva V, Garrote J, Benito G, Calle M, Lucía A, et al. Effects of sediment transport on flood hazards: Lessons learned and remaining challenges. Geomorphology 2024;446:Article No. 108976.

Wang Y, Jiang R, Xie J, Zhao Y, Yan D, Yang S. Soil and water assessment tool (SWAT) model: A systemic review. Journal of Coastal Research 2019;93:22-30.

Yohannes H, Argaw M, Seifu W. Impact of land use/land cover change on surface water hydrology in Akaki River catchment, Awash Basin, Ethiopia. Physics and Chemistry of the Earth, Parts A/B/C 2024;135:Article No. 103690.